HHS Public Access

Author manuscript

Neurochem Int. Author manuscript; available in PMC 2023 December 01.

Published in final edited form as:

Neurochem Int. 2022 December ; 161: 105436. doi:10.1016/j.neuint.2022.105436.

The interplay between MMP-12 and t-PA in the brain after ischemic stroke

Siva Reddy Challa[a,b,1], **Koteswara Rao Nalamolu**[a,1], **Casimir A. Fornal**[a], **Adithya Mohandass**[a], **Justin P. Mussman**[a], **Claire Schaibley**[a], **Aanan Kashyap**[a], **Vinay Sama**[a], **Billy C. Wang**[a,c,d], **Jeffrey D. Klopfenstein**[a,e,f], **David M. Pinson**[g], **Adinarayana Kunamneni**[h], **Krishna Kumar Veeravalli**[a,c,e,i,*]

[a]Department of Cancer Biology and Pharmacology, University of Illinois College of Medicine at Peoria, Peoria, Illinois, USA

[b]Department of Pharmacology, KVSR Siddhartha College of Pharmaceutical Sciences, Vijayawada, Andhra Pradesh, India

[c]Department of Pediatrics, University of Illinois College of Medicine at Peoria, Peoria, Illinois, USA

[d]Children's Hospital of Illinois, OSF HealthCare Saint Francis Medical Center, Peoria, Illinois, USA

[e]Department of Neurosurgery, University of Illinois College of Medicine at Peoria, Peoria, Illinois, USA

[f]Illinois Neurological Institute, OSF HealthCare Saint Francis Medical Center, Peoria, Illinois, USA

[g]Department of Health Sciences Education and Pathology, University of Illinois College of Medicine at Peoria, Peoria, Illinois, USA

[h]Department of Medicine, Mayo Clinic, Jacksonville, Florida, USA

[i]Department of Neurology, University of Illinois College of Medicine at Peoria, Peoria, Illinois, USA

Abstract

Tissue-type plasminogen activator (t-PA) expression is known to increase following transient focal cerebral ischemia and reperfusion. Previously, we reported downregulation of t-PA upon suppression of matrix metalloproteinase-12 (MMP-12), following transient focal cerebral ischemia and reperfusion. We now present data on the temporal expression of t-PA in the brain after transient ischemia, as well as the interaction between MMP-12 and t-PA, two proteases

*Corresponding author. Krishna Kumar Veeravalli PhD, Associate Professor, Department of Cancer Biology and Pharmacology, University of Illinois College of Medicine at Peoria, 1 Illini Dr., Peoria, IL 61605, USA, krishnav@uic.edu (K.K. Veeravalli).

[1]Shared first authorship.

Author statement

KKV, JDK, and DMP contributed to conceptualization, funding acquisition, and supervision. KKV, SRC, KRN, CAF, and BCW were involved in animal surgeries and care. SRC, KRN, CAF, AM, JPM, CS, VS, AK (Aanan Kashyap), and AK (Adinarayana Kunamneni) were involved in the methodology, investigation, and acquisition of data. KKV, CAF, SRC, and AK (Adinarayana Kunamneni) performed data analysis and interpretation. KKV prepared, and CAF edited the manuscript. All the authors reviewed and approved the final manuscript.

Declaration of interests

The authors declare no potential conflicts of interest.

Appendix A. Supplementary data

Supplementary data is available for this article.

associated with the breakdown of the blood-brain barrier (BBB) and ischemic brain damage. We hypothesized that there might be reciprocal interactions between MMP-12 and t-PA in the brain after ischemic stroke. This hypothesis was tested using shRNA-mediated gene silencing and computational modeling. Suppression of t-PA following transient ischemia and reperfusion in rats attenuated MMP-12 expression in the brain. The overall effect of t-PA shRNA administration was to attenuate the degradation of BBB tight junction protein claudin-5, diminish BBB disruption, and reduce neuroinflammation by decreasing the expression of the microglia/macrophage pro-inflammatory M1 phenotype (CD68, iNOS, IL-1β, and TNFα). Reduced BBB disruption and subsequent lack of infiltration of macrophages (the main source of MMP-12 in the ischemic brain) could account for the decrease in MMP-12 expression after t-PA suppression. Computational modeling of *in silico* protein-protein interactions indicated that MMP-12 and t-PA may interact physically. Overall, our findings demonstrate that MMP-12 and t-PA interact directly or indirectly at multiple levels in the brain following an ischemic stroke. The present findings could be useful in the development of new pharmacotherapies for the treatment of stroke.

Keywords

ischemia; reperfusion; matrix metalloproteinase-12; tissue-type plasminogen activator; blood-brain barrier; inflammation

1. Introduction

Worldwide, stroke remains the leading cause of death and disability. Ischemic stroke, which occurs due to the occlusion of cerebral blood arteries, accounts for about 87% of all strokes [1]. The two FDA-approved recanalization treatments, endovascular thrombectomy and thrombolysis drug therapy with tissue-type plasminogen activator (t-PA), terminate ischemia and restore blood flow, which is known as reperfusion. Transient cerebral ischemia followed by reperfusion leads to the upregulation of several matrix metalloproteinases (MMPs) in the ischemic brain [2,3]. The elevated MMPs damage essential components of the neurovascular matrix and blood-brain barrier (BBB), resulting in BBB leakage, leukocyte infiltration, brain edema, and hemorrhage [4]. MMPs also induce brain cell death by disrupting cell-matrix signaling and homeostasis [5,6]. We previously studied the temporal expression of all MMPs in the brain following transient cerebral ischemia and reperfusion. We discovered that MMP-12 upregulation was many times higher than any other MMP [2,3]. MMP-12 knockdown using shRNA-mediated gene silencing attenuated ischemic brain damage, at least in part, by reducing the degradation of tight junction proteins and thereby the BBB disruption, MMP-9 upregulation, apoptosis, neuroinflammation, and myelin basic protein degradation [2,7]. Attenuating MMP-12 expression in the brain promotes post-stroke neurological and functional recovery [8].

Within these experiments, we observed an increase in the protein expression of tissue-type plasminogen activator (t-PA) in the brain both during the ischemic period and following reperfusion [7]. Several prior studies have reported an increase in t-PA activity and expression in the ischemic brain [9–11]. Primary sources of t-PA in the brain include endothelial cells of cerebral microvessels, neurons, and local microglia [12,13]. Animal and

human studies indicate that t-PA increases the expression and activity of MMPs, especially MMP-9, which is well known for its role in post-ischemic BBB disruption [14–20]. We found that suppressing MMP-12 following acute cerebral ischemia reduces t-PA expression in the brain [7].

The temporal expression profile of t-PA in the brain following transient cerebral ischemia and reperfusion has not been previously studied. Therefore, in this investigation, we examined the expression of t-PA in the ischemic brain during the first week following reperfusion. Additionally, the interplay between MMP-12 and t-PA, two proteases implicated in ischemic brain damage, remains largely unknown. We hypothesized that there may be direct or indirect reciprocal interactions between MMP-12 and t-PA in the brain following an ischemic stroke. To test this idea, two different approaches (functional and simulated) were used: shRNA-mediated gene silencing to determine whether t-PA knockdown affects MMP-12 expression in an animal model of ischemic stroke and computational modeling to determine whether physical interactions exist between MMP-12 and t-PA. Our findings suggest that MMP-12 and t-PA interact functionally in the brain following an ischemic stroke, with one suppressing the expression of the other. *In silico* analysis uncovered multiple molecular sites where the two proteases may interact directly and potentially influence each other's activity

2. Materials and methods

2.1. Ethics and compliance statement

As stated in the *Guide for the Care and Use of Laboratory Animals* (Publication no. 86–23 revised, National Institutes of Health, U.S. Department of Health and Human Services), all animal experiments were planned and conducted in accordance with the scientific, humane, and ethical principles. The Institutional Animal Care and Use Committee (IACUC) of the University of Illinois College of Medicine Peoria approved all surgical procedures as well as pre- and post-operative animal care. All animal procedures conducted were in accordance with the IACUC-approved animal protocol. In addition, studies conducted and reported were in compliance with the *"Animal Research: Reporting of In Vivo Experiments"* guidelines [21]. The Institutional Biosafety Committee (IBC) of the University of Illinois College of Medicine Peoria approved the synthesis and isolation of plasmids containing shRNAs (control shRNA and t-PA shRNA) inserted in pSilencer™ 4.1-CMV neo vector (Ambion, Austin, TX) from bacterial cultures and their use for several *in vitro* and *in vivo* experiments in our laboratory. The development and production of plasmids and their handling by research personnel were in compliance with the IBC-approved protocol.

2.2. Transient focal cerebral ischemia induction in rats

A total of 94 healthy young (2–3 months old) male Sprague-Dawley rats were used in this study. Animals were procured (Envigo Laboratories, USA) and housed in the Laboratory Animal Care Facility at the University of Illinois College of Medicine Peoria. The housing conditions included a 12 h light/dark cycle, controlled temperature and humidity, and free access to food and water. Animals were randomly assigned to the following experimental groups: Sham, Untreated (no treatment), control shRNA treated, and t-PA shRNA treated

(Supplementary table 1). To induce ischemia, animals were subjected to a suture model right middle cerebral artery occlusion (MCAO) as described recently by our group [22]. Removal of the monofilament suture at a designated time (1.5 h or 2 h) after MCAO constituted reperfusion. Post-surgical care was provided following *"Ischemia Models: Procedural Refinements Of in Vivo Experiments"* guidelines [23]. Animals were euthanized at different time points after ischemia and their brain tissues were collected and subjected to multiple experimental methods as described in the subsequent sections.

2.3. Design, construction, and synthesis of t-PA shRNA plasmids

We designed, constructed, and synthesized plasmids expressing t-PA shRNA (TPAsh) specifically to silence the gene expression of t-PA. We used pSilencer™ 4.1-CMV neo vector obtained from Ambion (Austin, TX) to construct t-PA shRNA along with a scrambled sequence shRNA (control shRNA), which served as a control. The target t-PA mRNA sequence (gtacatagtccataaggaatt) was chosen and used to design the inverted repeat t-PA shRNA sequences (Supplementary Fig. 1). The inverted repeat sequences synthesized for t-PA were laterally symmetrical, causing them to be self-complementary with a 9 base pair mismatch in the loop region. The oligonucleotides/ultramers were annealed, and the annealed product was ligated to the vector at the BamHI and HindIII sites in accordance with the manufacturer's instructions. Scrambled sequence shRNAs were also prepared in a similar manner. The resultant vectors were transformed into chemically competent E. coli cells (JM109 competent cells) and cultured overnight. Plasmids expressing t-PA shRNA or control shRNA were synthesized from the overnight bacterial culture using QIAGEN plasmid mini kit (Qiagen, USA) in accordance with the manufacturer's protocol. Positive clones confirmed by gene sequencing analysis at the University of Illinois at Urbana-Champaign were used in this study.

2.4. Plasmid isolation, preparation of nanoparticle formulation, and treatment

The positive clones of t-PA shRNA and control shRNA were inoculated into the sterilized Luria-Bertani media and cultured overnight at 37 °C using an orbital shaker. After 16 hours, the culture was centrifuged at 6000 g for 15 min at 4 °C to collect the pellet. The plasmid from the pellet was extracted using a QIAGEN plasmid maxi kit (Qiagen, USA) in accordance with the manufacturer's protocol. The obtained plasmids were stored at −20 °C until use in formulation preparation. The t-PA shRNA treated or control shRNA plasmids were formulated as nanoparticles, which are small enough to diffuse into tissues and enter cells by endocytosis. The nanoparticle formulation was prepared using the *in vivo*-jetPEI reagent (Polyplus transfection, Illkirch, France) in accordance with the manufacturer's instructions. Nanoparticle formulations of t-PA shRNA or control shRNA plasmids were administered (1 mg/kg) intravenously via tail vein to rats within 30 min of reperfusion.

2.5. Cell culture and transfection conditions

PC12 rat pheochromocytoma and C6 rat glioma cell lines were obtained from the American Type Culture Collection (ATCC) and cultured in accordance with the manufacturer's protocol. Cells were maintained in ATCC-formulated F-12K medium supplemented with 2.5% fetal bovine serum and 15% horse serum in a humidified atmosphere containing 5% CO_2 at 37°C. The cells (~150,000) were transfected with either t-PAsh or control

shRNA using X-treme GENE HP DNA Transfection Reagent (Roche Diagnostics GmbH, Mannheim, Germany) as per the manufacturer's instructions. After transfection, cells were incubated in a serum-containing medium for a minimum of 60 h.

2.6. RT-PCR analysis and agarose gel electrophoresis

Total RNA was extracted from PC12/C6 cells and rat brain tissues using TRIzol reagent (Invitrogen, Carlsbad, USA). One μg of total RNA from each sample was reverse transcribed to cDNA using the *iScript cDNA Synthesis Kit* (Bio-Rad Laboratories, USA) in accordance with the manufacturer's instructions. RT-PCR analysis was performed with diluted cDNAs (1:10) obtained from various samples, diluted primers (Supplementary table 2) (1:10), and the GoTaq® Green Master Mix (Promega, USA) in accordance with the manufacturer's protocol. RT-PCR was performed in a C1000 Touch Thermo cycler (Bio-Rad Laboratories, USA) using the following PCR cycle: [95°C for 5 min, (95°C for 30 sec, 58–60°C for 30 sec, 72°C for 30 sec) × 35 cycles, and 72 °C for 5 min]. RT-PCR products were resolved on a 2% agarose gel, stained with ethidium bromide, and visualized under UV light. The mRNA expression of the house-keeping gene β-actin was used to normalize the mRNA expression of t-PA. The mRNA expression of t-PA as compared to the expression of β-actin across various groups was quantified using the ImageJ analysis (NIH) software.

2.7. Quantitative real-time PCR analysis

Real-time PCR analysis was performed using the SYBR Green method. The reaction setup for each diluted cDNA sample (1:10) was assembled using the iTaq Universal SYBR Green Supermix (Bio-Rad Laboratories, USA) per the manufacturer's instructions. The forward and reverse primer sequences (1:10 dilution in nuclease-free water) of target genes are listed in Supplementary table 2. Samples were subjected to the following PCR cycle: [95°C for 5min, (95 °C for 30 sec, 57–61 °C for 30 sec, 72 °C for 30 sec) × 40 cycles, and 72 °C for 5 min] in an iCycler IQ (Multi-Color Real-Time PCR Detection System; Bio-Rad Laboratories, Hercules, California, USA). Data was collected and recorded using the iCycler IQ software (Bio-Rad Laboratories, USA) and expressed as a function of the threshold cycle (Ct), representing the number of cycles at which the fluorescent intensity of the SYBR Green dye is significantly above that of the background fluorescence. β-actin or *18S* rRNA served as housekeeping genes or internal standards. Relative quantification of gene expression was normalized to *18S* rRNA or β-actin. The fold change in target gene expression in the test sample relative to the control sample was computed using the formula 2^(ΔCt of control)/2^(ΔCt of test).

2.8. Immunoblot analysis

Immunoblot analysis was performed using the cell lysates obtained from various *in vitro* (PC12 and C6 cells) and *in vivo* experimental conditions. Protein samples were subjected to immunoblot analysis using primary antibodies (Supplementary table 3) followed by HRP-conjugated secondary antibodies. Immunoreactive bands were visualized using chemiluminescence ECL Western blotting detection reagents (Bio-Rad Laboratories, USA). Bands were quantified using NIH ImageJ analysis software and normalized to the loading control GAPDH or β-actin.

2.9. Immunofluorescence analysis

Anesthetized rats were perfused with PBS followed by 4% buffered formaldehyde solution. Brains were cryoprotected with 30% sucrose and embedded in optimal cutting temperature compound before sectioning on a cryostat. Coronal brain sections (40 μm thick) containing the caudate nucleus at approximately bregma 0.2 mm were subjected to heat-induced epitope retrieval (10 mM Citric acid, pH 6.0; 100°C for 10 min) using a commercial steamer. Sections were permeabilized with Triton X-100, blocked with 5% normal goat serum, incubated overnight at 4°C with a mouse monoclonal anti-MMP12 antibody (sc-390863, Santa Cruz Biotechnology, Dallas, TX) at 1:250 dilution, and then incubated with Alexa Fluor 488-conjugated goat anti-mouse IgG secondary antibody (A-11001; Invitrogen, Carlsbad, CA), 1:500 dilution, for 3 h at room temperature in the dark. Sections were subsequently counterstained with 4’,6-diamidino-2-phenylindole (DAPI) to visualize cell nuclei. The slides were cover slipped and later viewed with a confocal laser scanning microscope (Olympus Fluoview FV3000). Digital images were obtained at 400× magnification using the same channel settings for all samples to allow direct comparison of fluorescence staining between treatment groups. Quantification of immunofluorescence was performed using NIH ImageJ 1.53e software by measuring integrated density (in arbitrary units) after background subtraction.

2.10. Evans blue dye extravasation assay

Three days after ischemia, rats from the appropriate treatment groups were assigned to study changes in BBB permeability using the Evans blue dye (EBD) extravasation method, as previously described [24]. A 2% EBD solution (prepared in 1xPBS and sterilized by passing through a 0.22 μm membrane filter) was slowly injected into rats at a dose of 4 mL/kg, i.v. via tail vein. The dye was allowed to circulate for 3 hours before animal perfusion. Rats were deeply anesthetized with sodium pentobarbital (~350 mg/kg, i.p.) and perfused intracardially with 1xPBS until the effusion became clear. The brain was then removed and divided along the midline into its two respective hemispheres. The ipsilateral and contralateral brain samples were collected separately and stored at −80 °C until assayed. The frozen brain samples were weighed, homogenized in 2.5 mL PBS, vortexed with 2.5 mL trichloroacetic acid (60%) for 2 min, centrifuged for 30 min at 1400×g, and cooled at 4°C for 10 min. Supernatants were collected, and the EBD absorbance was measured at 610 nm using a microplate spectrophotometer. For each brain hemisphere, the EBD concentration was determined using a standard curve obtained from known amounts of EBD and expressed as micrograms per gram of wet brain weight. In addition, the EBD ratio for each animal was calculated using the following formula: EBD Ratio = EBD concentration in the ipsilateral brain / EBD concentration in the contralateral brain. A ratio greater than one indicates a leakier BBB on the infarct side compared to the non-infarct side.

2.11. Computational modeling

An advanced computational protocol was used to determine the interactions between rat t-PA and MMP-12 proteins. For homology modeling, we used the Iterative Threading Assembly Refinement (I-TASSER) server for predicting the 3D structure models of protein molecules from amino acid sequences [25]. The predicted structural models

were validated using high-resolution protein structure refinement [(Protein refinement module, Schrodinger-Prime module, Biologics suite, Schrodinger 2021–1 (Schrödinger, LLC, New York, NY, 2021)], ModRefiner, and fragment-guided molecular dynamics (FG-MD) simulation [26].

The refined models were docked according to the Fast Fourier Transform (FFT)-based program and PIPER [27]. The t-PA-MMP-12 docking was modeled using the PIPER protein-protein docking program in the BioLuminate product [28]. The largest cluster size with minimal local energy and a near-native state of the protein conformation was chosen. Docking results were validated using the 2D protein-protein interaction analysis tool of Schrödinger suite 2021–1 software. An interactive map was studied to identify the chemical nature of the interactions such as hydrogen bonds, pi-pi interaction, side-chain bonds, and backbone hydrogen bonds. Protein–protein interaction maps were also used to predict the position and interacting amino acids of both the proteins.

Molecular dynamics (MD) simulation studies for the selected docked poses were carried out by the Desmond module of Schrödinger software with OPLS4 force field [29]. The protein-ligand complex was embedded in a predefined TIP3P water model in the orthorhombic box [30]. The box volume was minimized, and the overall system charge was neutralized by adding Na^+ or Cl^- ions and 0.15 mM NaCl to construct near-physiological conditions. The temperature and pressure were kept constant at 300 K and 1.01325 bar throughout the simulation using a Nose-Hoover thermostat and Martyna-Tobias-Klein barostat methods [31,32]. The simulations were performed for >100 ns using NPgammaT ensembles for proteins and membranes ensemble considering the number of atoms, pressure, and timescale [33]. During simulations, long–range electrostatic interactions were calculated using the Particle–Mesh–Ewald method and the whole ensemble was constructed as a rigid body packing and relaxed gradually at 1.2 kilojoules of energy during the simulations [33]. The amino acid energy contributions that were obtained from the prime molecular mechanics-generalized born surface area (MM-GBSA) calculation were used to elucidate the key amino acids critical for protein-protein interaction.

2.12. Exclusion criteria

Animals that did not exhibit a neurological severity score of 8 or above after ischemia and reperfusion were excluded from the study. Additionally, animals with postmortem evidence of hemorrhage around the MCA were excluded from the study. Data obtained from animals that died during the study period and data identified as outliers by the Grubbs test were excluded from analysis.

2.13. Statistical analysis

Statistical analyses of the data was performed using GraphPad Prism 8.4.3 for Windows. For each experiment, the quantitative data was tested for normality and equality of variances. On the basis of the number of groups present in each experiment and the outcome of the normality and variance tests, appropriate statistical tests (described in figure legends) were used to analyze the data. Differences between groups were considered significant at $p < 0.05$. All data are expressed as mean ± SEM.

3. Results

3.1. Increased t-PA expression in the brain following an ischemic stroke

Transient focal cerebral ischemia increased t-PA mRNA expression (2.8 fold over sham) in the ipsilateral brains of rats on post-reperfusion day 1 (Fig. 1A). The duration of this increase in t-PA mRNA expression was then determined. We observed elevated t-PA mRNA expression (2.4 fold over sham on day 3 and 3.4 fold over sham on day 5) for up to five days after reperfusion. The increase in t-PA expression was statistically significant on post-reperfusion days 1 ($p = 0.0002$), 3 ($p = 0.0036$), and 5 ($p < 0.0001$) but not on day 7. The expression of t-PA mRNA on post-reperfusion day 7 was comparable to that of the sham group.

3.2. t-PA shRNA treatment is effective in reducing t-PA expression in vitro and in vivo

TPA shRNA treatment decreased t-PA mRNA expression by 38% in PC12 cells and 68% in C6 cells compared to untreated cells (Supplementary Fig. 2A). In PC12 cells, the t-PA mRNA expression in the control shRNA transfected cells was not significantly different from that in untreated cells, whereas it was significantly decreased ($p = 0.0011$) in the t-PA shRNA transfected cells. In C6 cells, the t-PA mRNA expression was not significantly different in the control shRNA transfected cells compared to untreated cells, but it was significantly decreased ($p = 0.0017$) in the t-PA shRNA transfected cells. The protein expression of t-PA was also decreased by 89% in PC12 cells transfected with t-PA shRNA compared to untreated cells (Supplementary Fig. 2B). The t-PA protein expression was significantly decreased ($p = 0.0449$) in the t-PA shRNA transfected PC12 cells, but was not significantly different from untreated cells in the control shRNA transfected cells.

In vivo, the expression of t-PA mRNA was increased (2.8 fold over sham) on post-reperfusion day 1 in the ipsilateral brains of untreated stroke-induced rats, but not in the t-PA shRNA treated stroke-induced animals (Fig. 1B). The increase in t-PA mRNA expression in the untreated group, but not in the t-PA shRNA treated group, was statistically significant ($p = 0.0094$) when compared to the sham group. Furthermore, t-PA shRNA treatment significantly ($p = 0.0038$) reduced the expression of t-PA mRNA in the ipsilateral brains of stroke-induced rats compared to untreated stroke-induced animals. Thus, t-PA shRNA administration completely prevented the increase in t-PA mRNA associated with ischemic stroke. Overall, the results obtained in PC12/C6 cell lines and stroke-induced rats validate the ability of t-PA shRNA to suppress t-PA expression *in vitro* and *in vivo*.

3.3. TPA shRNA treatment suppresses the expression of MMP-12

The neurological assessment of stroke severity, as determined by the mNSS, 2 to 4 hours after reperfusion revealed scores of 9.83 ± 0.72 for the untreated and 10.00 ± 0.85 for the t-PA shRNA treated groups assigned for real-time PCR analysis. There was no statistically significant difference in scores between the untreated and t-PA shRNA treated groups. These results suggest that the severity of stroke in both groups of animals was the same.

The expression of MMP-12 mRNA in the ischemic brain on post-reperfusion day 1 was decreased by 93% in the t-PA shRNA treated group compared to the untreated group

(Fig. 2A). Statistical analysis revealed that the decrease in MMP-12 mRNA expression was significant ($p = 0.0037$). In addition, 14 days after reperfusion, immunofluorescence analysis showed a significant expression of MMP-12 protein in the ipsilateral brain hemisphere relative to the contralateral brain hemisphere in both the control shRNA and, to a lesser extent, the t-PA shRNA treated groups (Fig. 2B). ImageJ analysis revealed that MMP-12 protein expression in the ipsilateral brain was increased in both experimental groups; however the expression was reduced by 69% in the t-PA shRNA treated group compared to the control shRNA treated group (Fig. 2C). Based on our method of analysis, we attribute the increase in MMP-12 fluorescence in the ipsilateral hemisphere of both experimental groups to an increase in the fluorescence area rather than the fluorescence intensity. The increase in MMP-12 expression in the ipsilateral brain hemisphere relative to the contralateral brain hemisphere was statistically significant in the control shRNA treated group ($p = 0.0019$), but not in the t-PA shRNA treated group. In addition, the decrease in MMP-12 expression in the t-PA shRNA treated group compared to the control shRNA treated group was statistically significant ($p = 0.0021$) in the ipsilateral hemisphere, suggesting that t-PA shRNA treatment reduces MMP-12 expression in the ischemic brain.

3.4. t-AP shRNA treatment protects the integrity of the blood-brain barrier

The extravasation of EBD was more evident in the ischemic brains of rats treated with control shRNA than in those treated with t-PA shRNA as determined by visual inspection (Fig. 3A). We then measured the concentration of EBD in the contralateral (non-ischemic) and ipsilateral (ischemic) brain hemispheres in both the control shRNA and t-PA shRNA groups. The EBD concentration in the contralateral hemisphere compared to the ipsilateral hemisphere for the control shRNA group was 0.51 μg/g and 3.83 μg/g, respectively, whereas the corresponding values for t-PA shRNA were 0.68 μg/g and 1.39 μg/g. These values represent a 7.5 fold increase in the control shRNA group and a 2.1 fold increase in the t-PA shRNA group. As expected, the concentration of EBD in the ipsilateral hemisphere of the brain decreased by 64% in the t-PA shRNA group compared to the control shRNA group. The increase in EBD concentration in the ipsilateral brain relative to the contralateral brain was statistically significant only in the control shRNA group ($p < 0.0001$), but not in the t-PA shRNA group. In addition, the concentration of EBD in the ipsilateral brain was significantly lower ($p < 0.0001$) in the t-PA shRNA group compared to the control shRNA group. Overall, these findings indicate that t-PA shRNA administration following an acute ischemic stroke in rats protects the brain against BBB disruption.

Claudin-5 is one of the BBB tight junction proteins. In rats subjected to acute focal cerebral ischemia and reperfusion, the protein expression of claudin-5 was decreased by 78% compared to sham controls (Fig. 3B). The protein expression of claudin-5 was increased by 3.4 folds in the t-PA shRNA treated group compared to the untreated group. Statistical analysis revealed a significant decrease in the expression of claudin-5 ($p < 0.0001$) in the untreated group relative to the sham group, as well as a significant increase in the expression of claudin-5 ($p = 0.0018$) in the t-PA shRNA treated group relative to the untreated group. As expected, there was no significant difference between the untreated and control shRNA treated groups in the protein expression of Claudin-5.

3.5. Elevated t-PA levels in the ischemic brain contribute to inflammation

In this particular study, if the mRNA expression of the target genes increased/decreased by less than 5 fold compared to sham, we did not consider the change in gene expression to be significant. As expected, transient focal cerebral ischemia increased the expression of microglia/macrophage M1 phenotype markers in the ipsilateral hemisphere of rats on post-reperfusion day 1, compared to the sham group (5.7 fold over sham for CD68, 6.9 fold over sham for iNOS, 7.4 fold over sham for IL-1β, 11.6 fold over sham for IL-6, and 6.6 fold over sham for TNFα) (Fig. 4A). The increase in these M1 markers was statistically significant when compared to the sham group (CD68: $p = 0.0011$; iNOS: $p = 0.0011$; IL-1β: $p = 0.0023$; IL-6: $p = 0.0029$; TNFα: $p < 0.0001$). Interestingly, the expression of these M1 markers was not significantly increased in the t-PA shRNA treated group compared to the sham group, except for IL-6 and TNFα (IL-6: $p = 0.0109$; TNFα: $p = 0.0019$), suggesting that suppression of brain t-PA after an ischemic stroke prevents the upregulation of pro-inflammatory M1 markers in the ipsilateral brain. The expression of IL-1β and TNFα was also significantly lower in the t-PA shRNA treated group compared to the untreated group (IL-1β: $p = 0.0489$; TNFα: $p = 0.0445$).

Despite a few statistically significant differences between experimental groups, none of the M2 markers (CD206, CD163, Arg1, IL-10, and TGFβ) showed an appreciable (> 5 fold) increase in mRNA expression in the ipsilateral brain hemisphere on post-reperfusion day 1, compared to the sham group (Fig. 4B). These results indicate that microglia/macrophages in the ischemic brain were much more polarized towards the classic pro-inflammatory M1 phenotype than the anti-inflammatory M2 phenotype on post-reperfusion day 1. The suppression of brain t-PA did not increase the expression of M2 markers in the ipsilateral brain.

With the exception of IL-6, the expression of all M1 and M2 markers remained unchanged in the contralateral brain hemisphere, indicating that the effect is local and specific to the ipsilateral brain (Supplementary Fig. 3). Statistical analysis revealed that the increase in IL-6 expression in the contralateral brain on post-reperfusion day 1 was significant ($p = 0.002$) compared to the sham group. These results indicate that the upregulation of IL-6 expression following an ischemic stroke has far reaching effects.

3.6. Physical interaction exists between MMP-12 and t-PA

The molecular dynamics simulation confirmed the docking prediction of rat MMP-12 and t-PA docking with a sufficiently large and highly stable interface, with amino acid side chain residues of t-PA forming electrostatic, aromatic, and hydrophobic interactions with MMP-12 counterparts (Fig.5 and Supplementary Figs. 4, 5, and 6). The t-PA protein formed 16 hydrogen bond interactions with MMP-12 residues Gln 65, Val 71, Arg 102, Arg 223, Asn 226, Asp 249, Ser 256, Val 262, Asn 264, Thr 276, and Gln 280, which comprise the active site of the enzyme. These results are comparable to the 2-dimensional and 3-dimensional structures of the MMP-12 and t-PA complex. The hydrogen bond interactions of the complex were elucidated to validate the binding of t-PA to MMP-12 protein predicted by the docking simulation studies. The number of hydrogen bonds between the t-PA and MMP-12 protein complex (acceptor/donor) was calculated and matched for identity with

the hydrogen bond residues predicted in the docking analysis (Supplementary table 4). The residues involved in hydrogen bonding during post-simulation analysis of trajectories were found to be the same as those contributing to hydrogen bonding during the docking analysis.

4. Discussion

This study demonstrates that t-PA expression in the brain is elevated for up to five days following transient focal cerebral ischemia and reperfusion, t-PA shRNA treatment is effective in reducing t-PA expression both *in vitro* and *in vivo*, and suppression of t-PA expression with t-PA shRNA treatment decreases MMP-12 expression in the brain. In addition, this study demonstrates that t-PA shRNA treatment prevents BBB tight junction protein degradation, reduces BBB disruption, and attenuates neuroinflammation. Our research also shows that MMP-12 and t-PA may interact physically.

Increased t-PA activity was initially observed in the ischemic brain (vessel wall and penumbra zone surrounding the necrotic area) in 1998 [9]. Further research showed that t-PA activity in the brain increases as early as six hours following ischemia [10]. More recently, we observed an increase in t-PA expression in the brains of rats both immediately following ischemia and one day after transient ischemia and reperfusion [7]. To our knowledge, no previous study has examined the temporal expression profile of t-PA in the brain following transient cerebral ischemia and reperfusion. We found a significant and sustained increase in t-PA mRNA expression in the brain for up to five days in this study, followed by a decline.

This is the first study to demonstrate the non-viral, nanoparticle-mediated delivery of t-PA shRNA expressing plasmids *in vitro* and *in vivo*. Treatment with t-PA shRNA effectively reduced the expression of t-PA in rat C6 and PC12 cells as well as in ischemia-induced rats. From a mechanistic standpoint, plasmid nanoparticles containing t-PA shRNA enter cells and produce t-PA siRNAs, which bind to and destroy t-PA mRNAs. We believe that t-PA shRNA plasmid nanoparticles administered intravenously penetrate the brain and endothelial cells of cerebral microvessels in rats, where they decrease the expression of t-PA mRNA. Although t-PA shRNA effectively reduces t-PA expression in the rat brain as intended, delivery of these shRNA particles intravenously may lead to widespread changes in the expression of the target gene. With respect to therapeutic efficacy, we previously found comparable effects in rats when the same dose of shRNA plasmids was delivered intravenously or specially in the brain [7]. Our future studies will investigate the effectiveness of brain-specific injections of t-PA shRNA plasmid particles (through internal carotid artery) immediately following transient cerebral ischemia and reperfusion.

Previously, we demonstrated that silencing the MMP-12 gene with MMP-12 shRNA decreases the expression of t-PA in the ischemic brain [7]. These findings suggested that elevated MMP-12 levels in the brain following an ischemic stroke may increase t-PA. The mechanisms underlying this effect are largely unknown. We hypothesize that t-PA may be released from brain and endothelial cells of cerebral microvessels as a result MMP-12-induced brain injury. In this study, suppressing t-PA expression with t-PA shRNA decreased

MMP-12 expression on post-reperfusion days 1 and 14. The elevated t-PA may enhance MMP-12 secretion and activation in the ischemic brain through plasmin formation [34,35].

Although many different types of brain cells express MMP-12 under ischemic conditions, the primary source of MMP-12 in the ischemic brain is infiltrating monocytes that become macrophages [2,36]. Before monocytes can enter the brain following an ischemic stroke, the BBB must be compromised. Our previous research demonstrated that the BBB is disrupted both immediately after transient ischemia and 24 hours after reperfusion [7]. In the present study, we extend these findings to show the extent of BBB disruption in the ischemic brain three days after acute ischemia and reperfusion. Because infiltrating macrophages are the main source of MMP-12 in the ischemic brain and t-PA shRNA treatment reduced the expression of MMP-12, we postulated that elevated t-PA in the ischemic brain contributes significantly to BBB disruption. Following an ischemic stroke, elevated brain t-PA can have both proteolytic (plasmin-mediated) and non-proteolytic effects on the brain. The evidence presented below indicates that t-PA has a clear and decisive role in BBB disruption following an ischemic stroke. Binding of t-PA to LDL receptor-related protein (LRP) initiates signaling to brain vascular endothelial cells that ultimately results in breakdown of the BBB [37]. In addition, t-PA increases MMP-9 expression in a non-proteolytic manner and converts pro-MMP-9 to active MMP-9 in a proteolytic manner (through plasmin) [16,19,38,39]. MMP-9 is a known culprit in BBB disruption during ischemia and after reperfusion. Consistent with our expectations, the extravasation of Evans blue dye into the ischemic brain was significantly reduced by t-PA shRNA treatment. This finding further confirms the deleterious effects of elevated t-PA levels on the breakdown of the BBB following an ischemic stroke.

Properties of the BBB are largely determined by the tight junction protein complexes, which contain membrane proteins like claudin-5 and occludin and membrane-associated cytoplasmic scaffold proteins like ZO-1 [40,41]. Claudin-5 is essential for maintaining the tight junction density, and ZO-1 acts as a scaffold to anchor claudin-5 to the actin cytoskeleton [42,43]. Tight junctions are maintained by the interaction of claudin-5 and occludin with ZO proteins (ZO-1, 2, and 3). The degradation of these proteins compromises the integrity of tight junctions and increases the permeability of the BBB [42,44]. The present study confirms that claudin-5 protein expression is downregulated in rats following transient ischemia and reperfusion, and further demonstrates that treatment with t-PA shRNA prevents this effect.

Previously we showed that suppressing MMP-12 prevented the degradation of claudin-5, occludin, and ZO-1 after transient ischemia and reperfusion and significantly reduced MMP-9 expression and activity [2,7]. The findings of this present study indicate that elevated t-PA in the brain after acute ischemia degrades tight junction proteins and disrupts the BBB, either directly or indirectly, by increasing MMP-12 expression and activity in the ischemic brain. The possibility of multiple direct physical interactions between MMP-12 and t-PA proteins was demonstrated in the present study using *in silico* computational modeling. We propose that a direct interaction of t-PA with MMP-12 might convert the inactive pro-form of MMP-12 into its active form.

The t-PA-generated plasmin recruits inflammatory cells such as macrophages (blood-borne monocytes) and microglia (brain resident macrophage population) to the site of injury by activating chemokines [45,46]. In addition, t-PA promotes the adherence of circulating monocytes to sites of inflammation and activates microglia [47,48]. The fibronectin finger domain at the N-terminus of t-PA is primarily responsible for microglial activation [48]. Transgenic mice that overexpress neuroserpin, a potent endogenous inhibitor of t-PA, had reduced microglial activation following an ischemic stroke [12]. These findings suggest that t-PA is essential for microglial activation following ischemia. Furthermore, t-PA mediates microglial polarization. In the ischemic brain, recruited microglia and infiltrating macrophages can be activated to the classical M1 phenotype or alternative M2 phenotype. When microglia/macrophages are activated to the M1 phenotype, pro-inflammatory cytokines are released, whereas the M2 phenotype has anti-inflammatory, neuroprotective, and repair properties [49–54]. Following an ischemic stroke, the M1 polarization of microglia was greater in neuroserpin-deficient animals than in wild-type mice, consistent with the idea that t-PA increases neuroinflammation [55].

In the present study, we observed a marked increase in the expression of M1 markers (CD68, iNOS, IL-1β, IL-6, and TNFα), specifically in the ipsilateral brain hemisphere (except for IL-6, which was also elevated in the contralateral brain), following transient focal cerebral ischemia. The observation that IL-6 levels are elevated in both the ischemic and contralateral brain tissues strongly suggests that IL-6 increases following an ischemic stroke are global rather than local. This is consistent with other studies that have shown an increase in IL-6 levels in the serum/plasma of acute stroke patients [56,57]. The finding that t-PA shRNA treatment reduces the expression of M1 markers suggests that elevated brain t-PA following an ischemic stroke contributes significantly to the severity of acute inflammation. Previously, we showed that suppressing MMP-12 following transient ischemia reduced TNFα expression in the ischemic brain [2]. As stated earlier, the findings of this study suggest that elevated t-PA in the brain following transient ischemia reduces neuroinflammation directly or indirectly by decreasing MMP-12 expression and activity in the ischemic brain. The expression of the healthy M2 phenotype in the ischemic brain usually peaks 3 to 5 days following ischemia. As expected, none of the M2 markers (CD206, CD163, Arg1, IL-10, and TGFβ) were appreciably increased at the early time point (day 1 after transient cerebral ischemia) in our study. Furthermore, t-PA shRNA treatment did not increase the expression of M2 markers.

Our findings could improve the safety and efficacy of recombinant t-PA therapy, which is known to disrupt the BBB and cause hemorrhagic transformation. Although t-PA is considered the gold standard for treating ischemic stroke, the vast majority of patients remain untreated due to its limited treatment window (the first 4.5 hours after stroke onset). Elevated t-PA levels in the brain after an ischemic stroke and intravenous recombinant t-PA treatment for blood clot dissolution both increase MMP-12 (and MMP-9 downstream) in the brain, which are mainly responsible for the breakdown of the BBB. Suppression of t-PA following acute ischemia decreased the expression of MMP-12 in the brain and protected the BBB by decreasing the degradation of tight junction proteins. Conversely, suppressing MMP-12 reduced t-PA expression [7]. Increased brain MMP-12 levels may contribute significantly to thrombolysis-associated hemorrhagic transformation, thereby limiting the

therapeutic window for recombinant t-PA therapy after ischemic stroke. Targeting brain t-PA after recanalization with shRNA, by reducing post-ischemic induction of t-PA in the brain and MMP-12 activation, may mitigate ischemic brain damage and the detrimental side effects of administering recombinant t-PA beyond its therapeutic window. Targeting MMP-12 may also provide similar therapeutic benefits as demonstrated by our recent study, although this approach may be less direct because MMP-12 is likely to act downstream of t-PA [8]. A possible advantage of targeting MMP-12 as opposed to t-PA is the transfection of peripheral monocytes/macrophages with MMP-12 shRNA. As the BBB deteriorates due to acute ischemia, a growing number of blood-borne monocytes enter the brain and differentiate into macrophages, the primary source of MMP-12 in the ischemic brain. The invading macrophages elevate MMP-12 levels and further exacerbate brain damage. However, this effect is negated by suppressing the MMP-12 gene.

Overall, our research clearly demonstrates that targeting t-PA following an ischemic stroke can prevent the induction of MMP-12 in the ischemic brain and reduce the severity of brain injury. According to our findings, MMP-12 and t-PA interact at different levels in the brain following an ischemic stroke, either directly or indirectly. The two proteins interact in such a way that one influences the other and vice versa. Our future studies in animals lacking the t-PA gene may confirm a number of these findings. The present findings could contribute to the development of new pharmacotherapies for the treatment of stroke.

Supplementary Material

Refer to Web version on PubMed Central for supplementary material.

Acknowledgments

We thank the National Institute of Neurological Disorders and Stroke of the National Institutes of Health and the OSF HealthCare Illinois Neurological Institute for providing financial assistance. We thank Erika Sung for her assistance with the formatting of the manuscript.

Funding

This work was supported by research grants from the National Institute of Neurological Disorders and Stroke of the National Institutes of Health under Award Number R01NS102573 and the OSF HealthCare Illinois Neurological Institute. The funders had no role in study design, data collection, analysis, interpretation, publication decision, or manuscript preparation. The content of this study is the sole responsibility of the authors and does not necessarily reflect the official position of the funders.

Abbreviations and Acronyms:

t-PA / TPA	tissue-type plasminogen activator
MMP	Matrix metalloproteinase
BBB	Blood-brain barrier
shRNA	Short hairpin ribonucleic acid
MCAO	Middle cerebral artery occlusion
PCR	polymerase chain reaction

PBS	Phosphate-buffered saline
DAPI	diamino phenylindole
EBD	Evans blue dye
iNOS	inducible nitric oxide synthase
IL	Interleukin
TNF	Tumor necrosis factor
Arg	Arginase
TGF	Transforming growth factor
CD	Cluster of Differentiation
LRP	Low-density lipoprotein receptor-related protein

References

[1]. Virani SS, Alonso A, Benjamin EJ, Bittencourt MS, Callaway CW, Carson AP, et al. Heart Disease and Stroke Statistics-2020 Update: A Report From the American Heart Association, Circulation. 141 (2020) e139–e596.10.1161/CIR.0000000000000757 [doi]. [PubMed: 31992061]

[2]. Chelluboina B, Warhekar A, Dillard M, Klopfenstein JD, Pinson DM, Wang DZ, et al. Post-transcriptional inactivation of matrix metalloproteinase-12 after focal cerebral ischemia attenuates brain damage, Sci.Rep 5 (2015) 9504.10.1038/srep09504 [doi]. [PubMed: 25955565]

[3]. Nalamolu KR, Chelluboina B, Magruder IB, Fru DN, Mohandass A, Venkatesh I, et al. Post-stroke mRNA expression profile of MMPs: effect of genetic deletion of MMP-12, Stroke Vasc.Neurol 3 (2018) 153–159.10.1136/svn-2018-000142 [doi]. [PubMed: 30294471]

[4]. Sandoval KE, Witt KA. Blood-brain barrier tight junction permeability and ischemic stroke, Neurobiol.Dis 32 (2008) 200–219.10.1016/j.nbd.2008.08.005 [doi]. [PubMed: 18790057]

[5]. Lee SR, Lo EH. Induction of caspase-mediated cell death by matrix metalloproteinases in cerebral endothelial cells after hypoxia-reoxygenation, J.Cereb.Blood Flow Metab 24 (2004) 720–727.00004647–200407000-00002 [pii]. [PubMed: 15241180]

[6]. Gu Z, Cui J, Brown S, Fridman R, Mobashery S, Strongin AY, et al. A highly specific inhibitor of matrix metalloproteinase-9 rescues laminin from proteolysis and neurons from apoptosis in transient focal cerebral ischemia, J.Neurosci 25 (2005) 6401–6408.25/27/6401 [pii]. [PubMed: 16000631]

[7]. Chelluboina B, Klopfenstein JD, Pinson DM, Wang DZ, Vemuganti R, Veeravalli KK. Matrix Metalloproteinase-12 Induces Blood-Brain Barrier Damage After Focal Cerebral Ischemia, Stroke. 46 (2015) 3523–3531.10.1161/STROKEAHA.115.011031 [doi]. [PubMed: 26534974]

[8]. Challa S, Nalamolu K, Fornal C, Wang B, Martin R, Olson E, et al. Therapeutic efficacy of matrix metalloproteinase-12 suppression on neurological recovery after ischemic stroke: Optimal treatment timing and duration, Front. Neurosci 16 (2022) 1012812. 10.33891/fnins.2022.1012812 [doi]. [PubMed: 36267234]

[9]. Wang YF, Tsirka SE, Strickland S, Stieg PE, Soriano SG, Lipton SA. Tissue plasminogen activator (tPA) increases neuronal damage after focal cerebral ischemia in wild-type and tPA-deficient mice, Nat.Med 4 (1998) 228–231.10.1038/nm0298-228 [doi]. [PubMed: 9461198]

[10]. Yepes M, Sandkvist M, Wong MK, Coleman TA, Smith E, Cohan SL, et al. Neuroserpin reduces cerebral infarct volume and protects neurons from ischemia-induced apoptosis, Blood. 96 (2000) 569–576.S0006–4971(20)72087–2 [pii]. [PubMed: 10887120]

[11]. Lemarchand E, Maubert E, Haelewyn B, Ali C, Rubio M, Vivien D. Stressed neurons protect themselves by a tissue-type plasminogen activator-mediated EGFR-dependent mechanism, Cell Death Differ. 23 (2016) 123–131.10.1038/cdd.2015.76 [doi]. [PubMed: 26068590]

[12]. Cinelli P, Madani R, Tsuzuki N, Vallet P, Arras M, Zhao CN, et al. Neuroserpin, a neuroprotective factor in focal ischemic stroke, Mol.Cell.Neurosci 18 (2001) 443–457.S1044–7431(01)91028–0 [pii]. [PubMed: 11922137]

[13]. Siao CJ, Fernandez SR, Tsirka SE. Cell type-specific roles for tissue plasminogen activator released by neurons or microglia after excitotoxic injury, J.Neurosci 23 (2003) 3234–3242.23/8/3234 [pii]. [PubMed: 12716930]

[14]. Asahi M, Wang X, Mori T, Sumii T, Jung JC, Moskowitz MA, et al. Effects of matrix metalloproteinase-9 gene knock-out on the proteolysis of blood-brain barrier and white matter components after cerebral ischemia, J.Neurosci 21 (2001) 7724–7732.21/19/7724 [pii]. [PubMed: 11567062]

[15]. Aoki T, Sumii T, Mori T, Wang X, Lo EH. Blood-brain barrier disruption and matrix metalloproteinase-9 expression during reperfusion injury: mechanical versus embolic focal ischemia in spontaneously hypertensive rats, Stroke. 33 (2002) 2711–2717.10.1161/01.str.0000033932.34467.97 [doi]. [PubMed: 12411666]

[16]. Sumii T, Lo EH. Involvement of matrix metalloproteinase in thrombolysis-associated hemorrhagic transformation after embolic focal ischemia in rats, Stroke. 33 (2002) 831–836.10.1161/hs0302.104542 [doi]. [PubMed: 11872911]

[17]. Horstmann S, Kalb P, Koziol J, Gardner H, Wagner S. Profiles of matrix metalloproteinases, their inhibitors, and laminin in stroke patients: influence of different therapies, Stroke. 34 (2003) 2165–2170.10.1161/01.STR.0000088062.86084.F2 [doi]. [PubMed: 12907822]

[18]. Montaner J, Molina CA, Monasterio J, Abilleira S, Arenillas JF, Ribo M, et al. Matrix metalloproteinase-9 pretreatment level predicts intracranial hemorrhagic complications after thrombolysis in human stroke, Circulation. 107 (2003) 598–603.10.1161/01.cir.0000046451.38849.90 [doi]. [PubMed: 12566373]

[19]. Lo EH, Broderick JP, Moskowitz MA. tPA and proteolysis in the neurovascular unit, Stroke. 35 (2004) 354–356.10.1161/01.STR.0000115164.80010.8A [doi]. [PubMed: 14757877]

[20]. Ning M, Furie KL, Koroshetz WJ, Lee H, Barron M, Lederer M, et al. Association between tPA therapy and raised early matrix metalloproteinase-9 in acute stroke, Neurology. 66 (2006) 1550–1555.66/10/1550 [pii]. [PubMed: 16717217]

[21]. Percie du Sert N, Hurst V, Ahluwalia A, Alam S, Avey MT, Baker M, et al. The ARRIVE guidelines 2.0: Updated guidelines for reporting animal research, J.Cereb.Blood Flow Metab 40 (2020) 1769–1777.10.1177/0271678X20943823 [doi]. [PubMed: 32663096]

[22]. Chelluboina B, Nalamolu KR, Mendez GG, Klopfenstein JD, Pinson DM, Wang DZ, et al. Mesenchymal Stem Cell Treatment Prevents Post-Stroke Dysregulation of Matrix Metalloproteinases and Tissue Inhibitors of Metalloproteinases, Cell.Physiol.Biochem 44 (2017) 1360–1369.10.1159/000485533 [doi]. [PubMed: 29186705]

[23]. Percie du Sert N, Alfieri A, Allan SM, Carswell HV, Deuchar GA, Farr TD, et al. The IMPROVE Guidelines (Ischaemia Models: Procedural Refinements Of in Vivo Experiments), J.Cereb.Blood Flow Metab 37 (2017) 3488–3517.10.1177/0271678X17709185 [doi]. [PubMed: 28797196]

[24]. Panahpour H, Farhoudi M, Omidi Y, Mahmoudi J. An In Vivo Assessment of Blood-Brain Barrier Disruption in a Rat Model of Ischemic Stroke, J.Vis.Exp (133). doi (2018) 10.3791/57156.10.3791/57156 [doi].

[25]. Yang J, Yan R, Roy A, Xu D, Poisson J, Zhang Y. The I-TASSER Suite: protein structure and function prediction, Nat.Methods 12 (2015) 7–8.10.1038/nmeth.3213 [doi].

[26]. Zhang J, Liang Y, Zhang Y. Atomic-level protein structure refinement using fragment-guided molecular dynamics conformation sampling, Structure. 19 (2011) 1784–1795.10.1016/j.str.2011.09.022 [doi]. [PubMed: 22153501]

[27]. Chuang GY, Kozakov D, Brenke R, Comeau SR, Vajda S. DARS (Decoys As the Reference State) potentials for protein-protein docking, Biophys.J 95 (2008) 4217–4227.10.1529/biophysj.108.135814 [doi]. [PubMed: 18676649]

[28]. Bhachoo J, Beuming T. Investigating Protein-Peptide Interactions Using the Schrodinger Computational Suite, Methods Mol.Biol 1561 (2017) 235–254.10.1007/978-1-4939-6798-8_14 [doi]. [PubMed: 28236242]

[29]. Harder E, Damm W, Maple J, Wu C, Reboul M, Xiang JY, et al. OPLS3: A Force Field Providing Broad Coverage of Drug-like Small Molecules and Proteins, J.Chem.Theory Comput 12 (2016) 281–296.10.1021/acs.jctc.5b00864 [doi]. [PubMed: 26584231]

[30]. Jorgensen WL, Chandrasekhar J, Madura JD, Impey RW, Klein ML Comparison of simple potential functions for simulating liquid water, J. Chem. Phys 79 (1983) 926.

[31]. Hoover WG. Canonical dynamics: Equilibrium phase-space distributions, Phys.Rev.A.Gen.Phys 31 (1985) 1695–1697.10.1103/physreva.31.1695 [doi]. [PubMed: 9895674]

[32]. Martyna GJ, Tobias DJ, Klein ML. Constant-Pressure Molecular-Dynamics Algorithms, J. Chem. Phys 101 (1994) 4177.

[33]. Ikeguchi M. Partial rigid-body dynamics in NPT, NPAT and NPgammaT ensembles for proteins and membranes, J.Comput.Chem 25 (2004) 529–541.10.1002/jcc.10402 [doi]. [PubMed: 14735571]

[34]. Carmeliet P, Moons L, Lijnen R, Baes M, Lemaitre V, Tipping P, et al. Urokinase-generated plasmin activates matrix metalloproteinases during aneurysm formation, Nat.Genet 17 (1997) 439–444.10.1038/ng1297-439 [doi]. [PubMed: 9398846]

[35]. Raza SL, Nehring LC, Shapiro SD, Cornelius LA. Proteinase-activated receptor-1 regulation of macrophage elastase (MMP-12) secretion by serine proteinases, J.Biol.Chem 275 (2000) 41243–41250.10.1074/jbc.M005788200 [doi]. [PubMed: 10993890]

[36]. Svedin P, Hagberg H, Mallard C. Expression of MMP-12 after neonatal hypoxic-ischemic brain injury in mice, Dev.Neurosci 31 (2009) 427–436.10.1159/000232561 [doi]. [PubMed: 19672072]

[37]. Yepes M, Sandkvist M, Moore EG, Bugge TH, Strickland DK, Lawrence DA. Tissue-type plasminogen activator induces opening of the blood-brain barrier via the LDL receptor-related protein, J.Clin.Invest 112 (2003) 1533–1540.10.1172/JCI19212 [doi]. [PubMed: 14617754]

[38]. Wang X, Lee SR, Arai K, Lee SR, Tsuji K, Rebeck GW, et al. Lipoprotein receptor-mediated induction of matrix metalloproteinase by tissue plasminogen activator, Nat.Med 9 (2003) 1313–1317.10.1038/nm926 [doi]. [PubMed: 12960961]

[39]. Kelly MA, Shuaib A, Todd KG. Matrix metalloproteinase activation and blood-brain barrier breakdown following thrombolysis, Exp.Neurol 200 (2006) 38–49.S0014–4886(06)00020–3 [pii]. [PubMed: 16624294]

[40]. Stamatovic SMKeep RF, Andjelkovic AV. Brain endothelial cell-cell junctions: how to “open” the blood brain barrier, Curr.Neuropharmacol 6 (2008) 179–192.10.2174/157015908785777210 [doi]. [PubMed: 19506719]

[41]. Luissint AC, Artus C, Glacial F, Ganeshamoorthy K, Couraud PO. Tight junctions at the blood brain barrier: physiological architecture and disease-associated dysregulation, Fluids Barriers CNS. 9 (2012) 23–8118-9–23.10.1186/2045-8118-9-23 [doi].

[42]. Furuse M, Itoh M, Hirase T, Nagafuchi A, Yonemura S, Tsukita S, et al. Direct association of occludin with ZO-1 and its possible involvement in the localization of occludin at tight junctions, J.Cell Biol 127 (1994) 1617–1626.10.1083/jcb.127.6.1617 [doi]. [PubMed: 7798316]

[43]. Itoh M, Furuse M, Morita K, Kubota K, Saitou M, Tsukita S. Direct binding of three tight junction-associated MAGUKs, ZO-1, ZO-2, and ZO-3, with the COOH termini of claudins, J.Cell Biol 147 (1999) 1351–1363.10.1083/jcb.147.6.1351 [doi]. [PubMed: 10601346]

[44]. Fanning AS, Jameson BJ, Jesaitis LA, Anderson JM. The tight junction protein ZO-1 establishes a link between the transmembrane protein occludin and the actin cytoskeleton, J.Biol.Chem 273 (1998) 29745–29753.10.1074/jbc.273.45.29745 [doi]. [PubMed: 9792688]

[45]. Ploplis VA, French EL, Carmeliet P, Collen D, Plow EF. Plasminogen deficiency differentially affects recruitment of inflammatory cell populations in mice, Blood. 91 (1998) 2005–2009.S0006–4971(20)54798–8 [pii]. [PubMed: 9490683]

[46]. Sheehan JJ, Zhou C, Gravanis I, Rogove AD, Wu YP, Bogenhagen DF, et al. Proteolytic activation of monocyte chemoattractant protein-1 by plasmin underlies excitotoxic neurodegeneration in mice, J.Neurosci 27 (2007) 1738–1745.27/7/1738 [pii]. [PubMed: 17301181]

[47]. Rogove AD, Siao C, Keyt B, Strickland S, Tsirka SE. Activation of microglia reveals a non-proteolytic cytokine function for tissue plasminogen activator in the central nervous system, J.Cell.Sci 112 (Pt 22) (1999) 4007–4016. [PubMed: 10547361]

[48]. Siao CJ, Tsirka SE. Tissue plasminogen activator mediates microglial activation via its finger domain through annexin II, J.Neurosci 22 (2002) 3352–3358.20026281 [doi]. [PubMed: 11978811]

[49]. Ding AH, Nathan CF, Stuehr DJ. Release of reactive nitrogen intermediates and reactive oxygen intermediates from mouse peritoneal macrophages. Comparison of activating cytokines and evidence for independent production, J.Immunol 141 (1988) 2407–2412. [PubMed: 3139757]

[50]. Goerdt S, Politz O, Schledzewski K, Birk R, Gratchev A, Guillot P, et al. Alternative versus classical activation of macrophages, Pathobiology. 67 (1999) 222–226.28096 [pii]. [PubMed: 10725788]

[51]. Kigerl KA, Gensel JC, Ankeny DP, Alexander JK, Donnelly DJ, Popovich PG. Identification of two distinct macrophage subsets with divergent effects causing either neurotoxicity or regeneration in the injured mouse spinal cord, J.Neurosci 29 (2009) 13435–13444.10.1523/JNEUROSCI.3257-09.2009 [doi]. [PubMed: 19864556]

[52]. Maroso M, Balosso S, Ravizza T, Liu J, Bianchi ME, Vezzani A. Interleukin-1 type 1 receptor/Toll-like receptor signalling in epilepsy: the importance of IL-1beta and high-mobility group box 1, J.Intern.Med 270 (2011) 319–326.10.1111/j.1365-2796.2011.02431.x [doi]. [PubMed: 21793950]

[53]. Durafourt BA, Moore CS, Zammit DA, Johnson TA, Zaguia F, Guiot MC, et al. Comparison of polarization properties of human adult microglia and blood-derived macrophages, Glia. 60 (2012) 717–727.10.1002/glia.22298 [doi]. [PubMed: 22290798]

[54]. Wyatt-Johnson SK, Herr SA, Brewster AL. Status Epilepticus Triggers Time-Dependent Alterations in Microglia Abundance and Morphological Phenotypes in the Hippocampus, Front.Neurol 8 (2017) 700.10.3389/fneur.2017.00700 [doi]. [PubMed: 29326654]

[55]. Gelderblom M, Neumann M, Ludewig P, Bernreuther C, Krasemann S, Arunachalam P, et al. Deficiency in serine protease inhibitor neuroserpin exacerbates ischemic brain injury by increased postischemic inflammation, PLoS One. 8 (2013) e63118.10.1371/journal.pone.0063118 [doi]. [PubMed: 23658802]

[56]. Nakase T, Yamazaki T, Ogura N, Suzuki A, Nagata K. The impact of inflammation on the pathogenesis and prognosis of ischemic stroke, J.Neurol.Sci 271 (2008) 104–109.10.1016/j.jns.2008.03.020 [doi]. [PubMed: 18479710]

[57]. Shaafi S, Sharifipour E, Rahmanifar R, Hejazi S, Andalib S, Nikanfar M, et al. Interleukin-6, a reliable prognostic factor for ischemic stroke, Iran.J.Neurol 13 (2014) 70–76. [PubMed: 25295149]

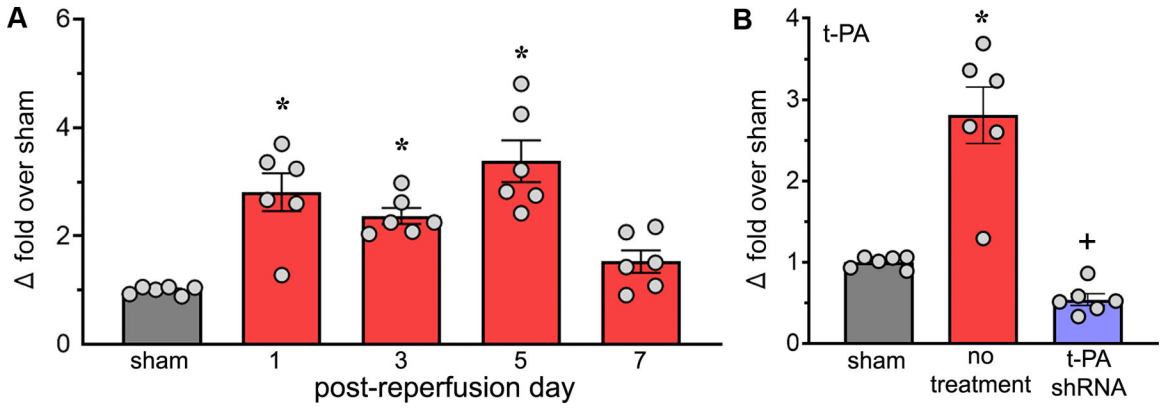

Fig. 1.

Stroke increases t-PA levels in the ischemic brain, and t-PA shRNA treatment is effective in reducing t-PA mRNA expression. (A) The expression of t-PA mRNA in the ipsilateral brain of rats subjected to 2-h focal cerebral ischemia followed by reperfusion. The column scatter plots show the quantified mRNA expression of t-PA, expressed as fold change over sham, in the ipsilateral brains of untreated stroke-induced rats on post-reperfusion days 1, 3, 5, and 7. *Statistical analysis*: One-way ANOVA followed by Dunnett's multiple comparisons test. *$p < 0.05$ vs Sham group. (B) The column scatter plots show the quantified mRNA expression of t-PA, expressed as fold change over sham, in the ipsilateral brains of untreated (no treatment) and t-PA shRNA treated stroke-induced rats on post-reperfusion day 1. *Statistical analysis*: Brown-Forsythe ANOVA followed by Dunnett's T3 multiple comparisons test. *$p < 0.05$ vs. Sham group. $^{+}p < 0.01$ vs. Untreated (no treatment) group.

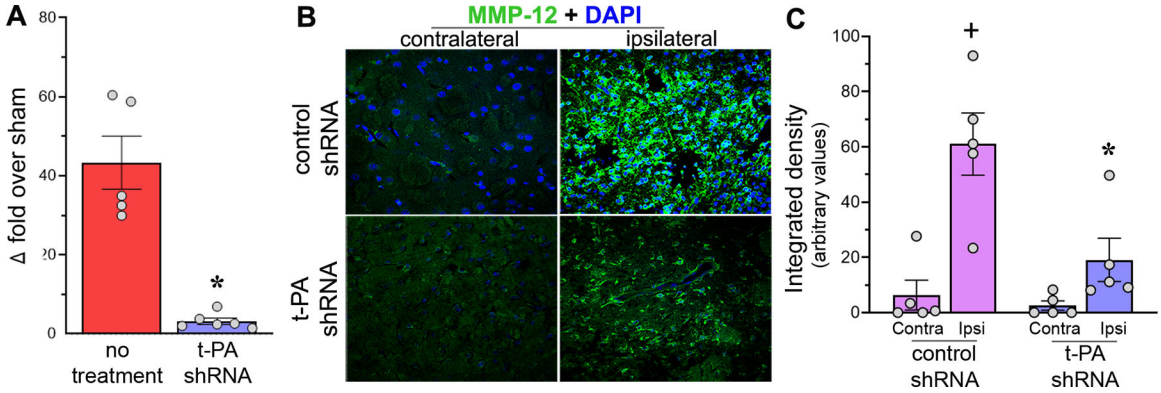

Fig. 2.

Effect of t-PA suppression on the expression of MMP-12. (A) The mRNA expression of MMP-12 in the ischemic brains of untreated and t-PA shRNA treated rats subjected to 2-h focal cerebral ischemia followed by reperfusion. The column scatter plot shows the quantified mRNA expression of MMP-12, expressed as fold change over sham, in the rat brains on post-reperfusion day 1. *Statistical analysis*: Unpaired *t* test with Welch's correction. $*p < 0.05$ vs Untreated group. (B) Images (400x) depicting MMP-12 protein expression (green fluorescence) in the ipsilateral and contralateral brains of control shRNA and t-PA shRNA treated stroke-induced rats on post-reperfusion day 14. Nuclei (blue fluorescence) were stained with DAPI. (C) The column scatter plot shows the integrated density of the quantified green fluorescence corresponding to MMP-12 expression. Contra, denotes the contralateral hemisphere of the brain; Ipsi, the ipsilateral hemisphere. *Statistical analysis*: Two-way repeated-measures ANOVA followed by Sidak's multiple comparisons test. $^{+}p < 0.05$ vs Contra (same experimental group). $*p < 0.05$ vs control shRNA treated group (same brain hemisphere).

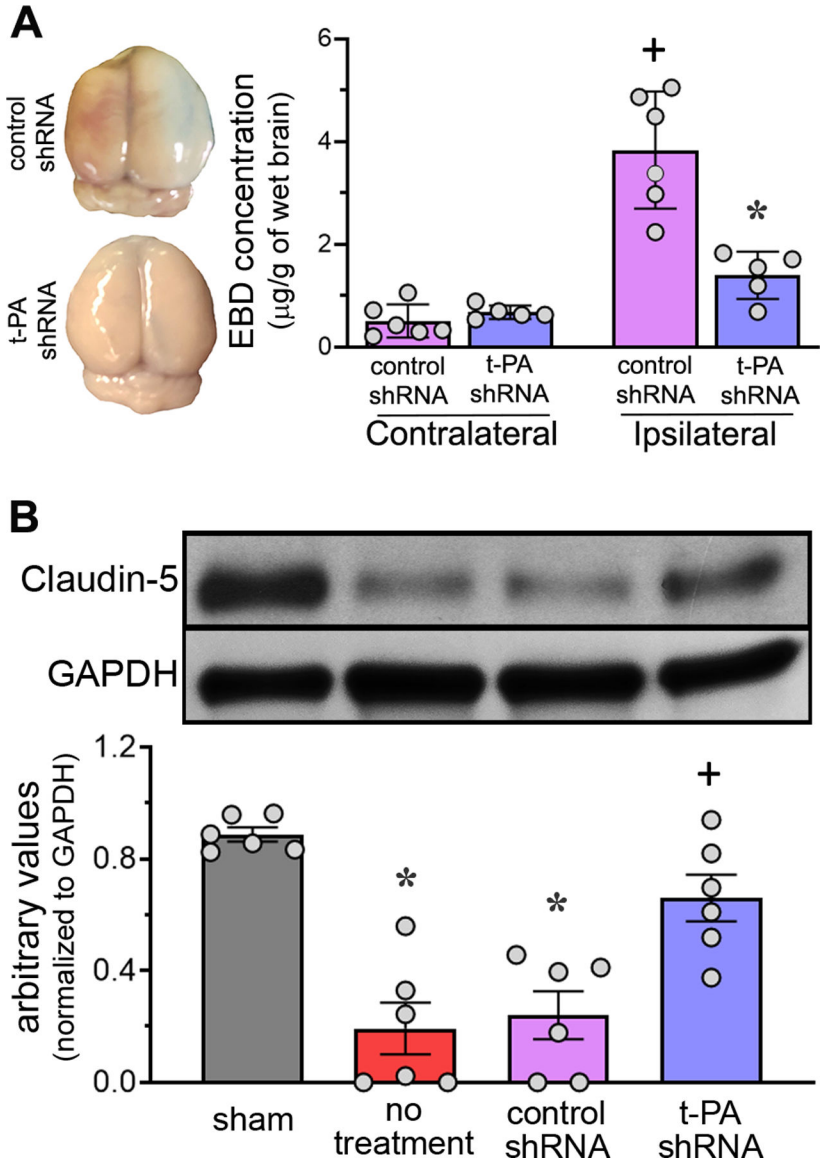

Fig. 3.

t-PA shRNA treatment preserves the integrity of the blood-brain barrier. (A) Representative photographs of the whole brain showing the contralateral and ipsilateral hemispheres of rats administered Evans blue dye (EBD) three days after 1.5-h focal cerebral ischemia followed by reperfusion. The column scatter plot shows the quantified concentration of EBD in the brains of rats treated with control shRNA and t-PA shRNA. *Statistical analysis*: Two-way repeated-measures ANOVA followed by Sidak's multiple comparisons test. $^{+}p < 0.05$ vs contralateral hemisphere (same experimental group). $*p < 0.05$ vs Control shRNA group (same brain hemisphere). (B) Representative immunoblots depicting the protein expression of claudin-5 in the ipsilateral brains of rats one day after 1.5-h focal cerebral ischemia and reperfusion. The column scatter plots show the quantified protein expression of claudin-5 normalized to the loading control GAPDH in sham, untreated, control shRNA treated, and t-PA shRNA treated stroke-induced rat brains on post-reperfusion day 1. *Statistical analysis*:

One-way ANOVA followed by Tukey's multiple comparisons test. *$p < 0.05$ vs Sham group. $^{+}p < 0.05$ vs Untreated (no treatment) group.

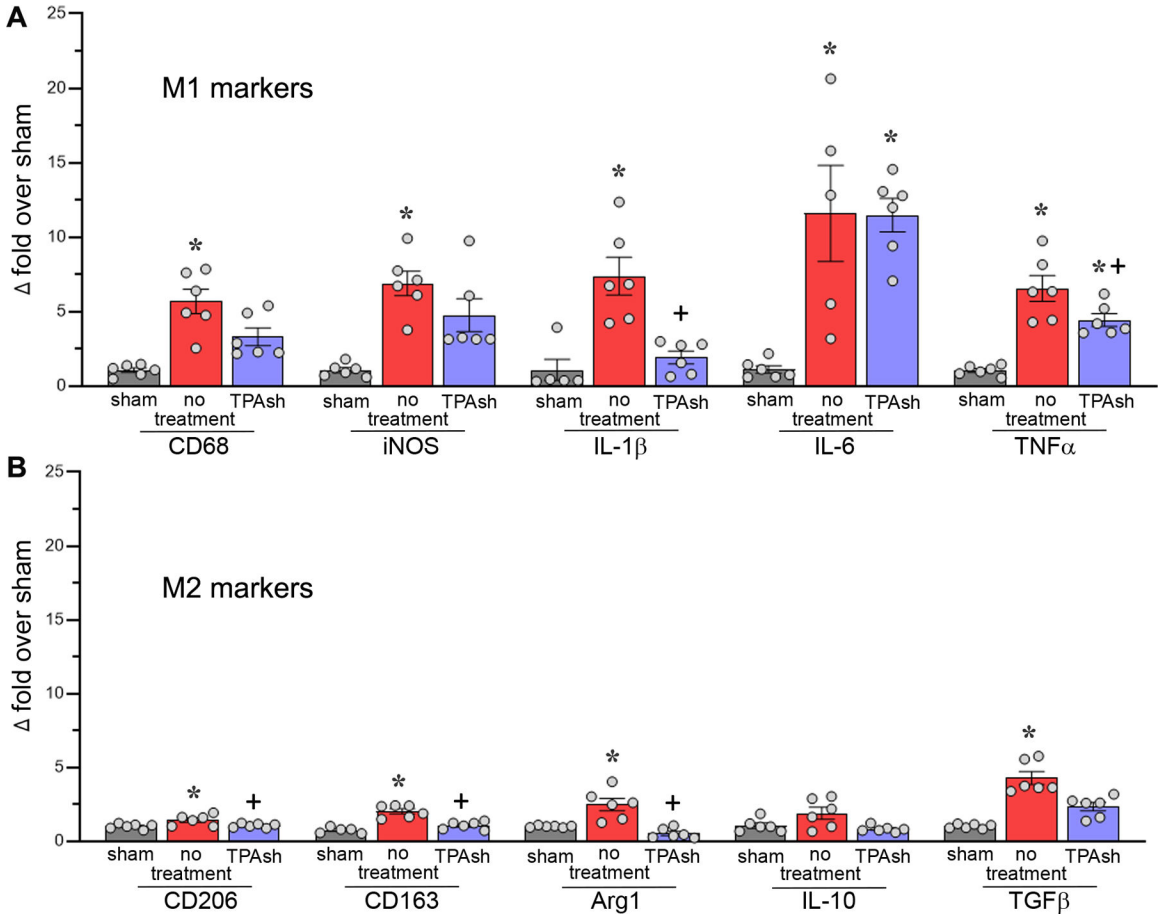

Fig. 4.

Effect of t-PA shRNA treatment on microglia/macrophage polarization dynamics in the brain following an ischemic stroke. The mRNA expression of M1 and M2 markers in the ipsilateral brains of rats subjected to 2-h focal cerebral ischemia and reperfusion. The column scatter plots show the quantified mRNA expression of the M1 markers CD68, iNOS, IL-1β, IL-6, and TNFα (A) and M2 markers CD206, CD163, Arg1, IL-10, and TGFβ (B), expressed as fold change over sham, in the ipsilateral brains of rats in the Untreated (no treatment) and t-PA shRNA (TPAsh) treated groups on post-reperfusion day 1. *Statistical analysis*: One-way ANOVA followed by Tukey's multiple comparisons test or Kruskal-Wallis test followed by Dunn's multiple comparisons test. $^{*}p < 0.05$ vs Sham group. $^{+}p < 0.05$ vs Untreated (no treatment) group.

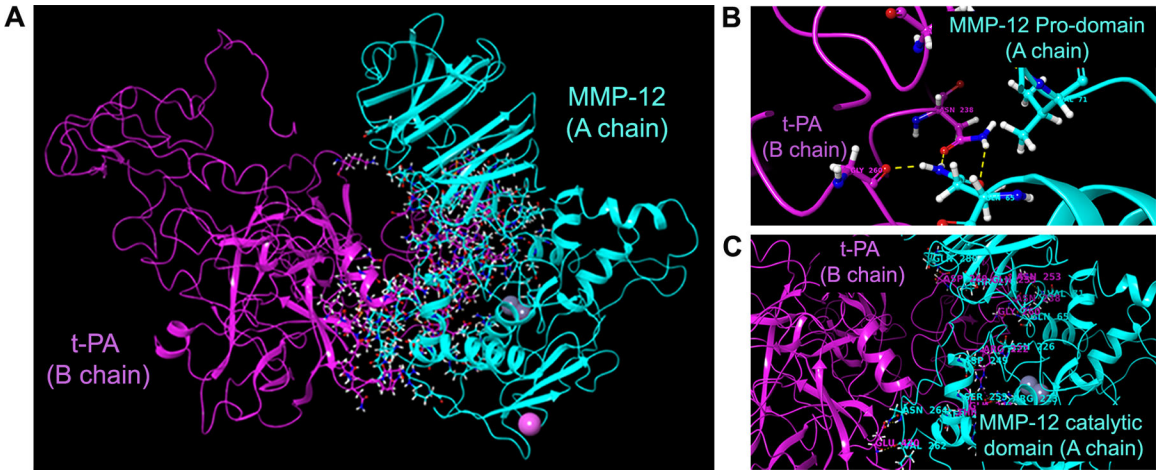

Fig. 5.

In silico analysis of a possible interaction between MMP-12 and t-PA (A) Amino acid side chain residue complements form the interface of rat t-PA with rat pro-MMP-12. (B and C) Binding poses of t-PA with MMP-12 sites (pro and catalytic domains), represented by hydrogen bonds at Gln 65, Val 71, Arg 102, Arg 223, Asn 226, Asp 249, Ser 256, Val 262, Asn 264, Thr 276, and Gln 280. The interaction diagram also depicts the van der Waals clash at Ser 253. All hydrogen bond interactions are shown as yellow dashed lines, all CH-O interactions as blue dashed lines, and all halogen interactions as purple dashed lines.